Powder Technology 254 (2014) 150–159

Contents lists available at ScienceDirect

Powder Technology

journal homepage: www.elsevier.com/locate/powtec

Numerical study of solid particle erosion in a cavity with different wall heights

Zhe Lin [a,b], Xiaodong Ruan [a,*], Zuchao Zhu [a,b], Xin Fu [a]

[a] State Key Laboratory of Fluid Power Transmission and Control, Zhejiang University, Zheda Road 38, Hangzhou, 310027, China
[b] The Province Key Laboratory of Fluid Transmission Technology, Zhejiang Sci-Tech University, 5 Second Avenue, Xiasha Higher Education Zone, Hangzhou, 310018, China

ARTICLE INFO

Article history:
Received 21 June 2013
Received in revised form 3 January 2014
Accepted 3 January 2014
Available online 11 January 2014

Keywords:
Cavity
Height difference
Solid particle erosion
Computational fluid dynamics

ABSTRACT

Ideal cavities face a high risk of erosion in relation to pneumatic conveying. To reduce erosion, we introduce a height difference in the cavity, with the leading wall higher than the aft wall. To improve the cavity structure, the URANS (SST)-DPM method is adopted to study the effect of height difference h on gas flow, particle distribution, and particle erosion of a horizontal ideal cavity. The simulation procedure is validated by comparing the computational fluid dynamics results with experimental results. The results of the gas flow modeling show that the shear layer impinges on the aft wall when h is relatively small, and re-attaches on the downstream bottom wall as h increases. The re-attachment length is initially identical to the cavity width, then increases uniformly with h. Results of the particle distribution simulations indicate that for a Stokes number (St) of 0.12, the particles are evenly distributed in the cavity, and the distribution is independent of h; for St = 1.2, dominated by the centrifugal force, the particles are mainly concentrated along the periphery of the main vortex when h is small. Owing to the variation of the main vortex, as h increases, more particles will fall down into the main vortex. For St = 9.1, where gravity is dominant, the particles collide on the aft wall and rebound into the cavity through the main vortex when h is small. Otherwise, particles will move forward and only a few particles appear in the cavity. We explored the erosion distribution on the downstream bottom walls and extracted and analyzed the initial erosion positions. We also investigate the erosion on the aft walls, and the results indicate that lowering the aft wall even slightly will significantly reduce erosion.

1. Introduction

An ideal cavity is a structural form created by sudden expansion and sudden contraction, where the leading wall and aft wall have the same height (Fig. 1). It is commonly found in piping components (such as double flat gate valves and connections) related to pneumatic conveying. When the carrier fluid contains particles, ideal cavities face a high risk of solid particle erosion which may result in equipment malfunctioning and even failure [1–5]. Thus, it is important to improve the erosion resistance of this structure based on two-phase flow analysis.

With the development of computer technology, numerical methods have been used for solving gas–solid flow problems, and predicting material erosion caused by particle impact [6–13]. The gas phase is solved by the Eulerian approach. By treating the particles as either a discrete phase or a continuum, two approaches are proposed for particle simulation, namely the Lagrangian approach and the Eulerian approach, respectively. In the Lagrangian approach, the detailed physical behavior of the particles can be obtained directly from the particle trajectories. However, in the Eulerian approach it is difficult to extract the particle impingement values from the Eulerian flow field. Therefore, although the Eulerian approach has been applied in erosion studies, it is more convenient to use the Lagrangian approach.

Solid particle erosion in the case of sudden expansion or sudden contraction has been analyzed in many studies [8,9,14–16]. The influence of diameter ratio and flow parameters (flow velocity, particle diameter, etc.) on erosion was investigated. However, only a few studies have been carried out on erosion of ideal cavities, namely those found in references [3,4]. Postlethwaite and Nesic [3] performed erosion tests of an ideal cavity by silica sand, showing that the cell wall geometry at the downstream leading edge is rounded by erosion. Changes in geometry resulted in lower erosion rates where rounding of the edge occurred. Wong et al. [4] examined and predicted the erosion characteristics of the surfaces of a vertically placed aluminum ideal cavity by using experimental and computational methods, and showed that the highest erosion rate occurs at the downstream leading edge. Thus, very limited information is available in the literature regarding the improvement of erosion resistance of this structure by flow analysis.

Since the alteration of the flow passage will change the gas–solid flowing states and modify the erosion pattern, we investigate an ideal cavity with a height difference where the leading wall is higher than the aft wall, for the purpose of erosion reduction. For structural improvement, the Eulerian–Lagrangian simulation method is used, and

* Corresponding author at: State Key Laboratory of Fluid Power Transmission and Control, Zhejiang University, China. Tel./fax: +86 571 8795 3395.
E-mail address: xdruan@zju.edu.cn (X. Ruan).

0032-5910/$ – see front matter © 2014 Elsevier B.V. All rights reserved.
http://dx.doi.org/10.1016/j.powtec.2014.01.002

the erosion is estimated from the obtained particle information. We discuss the influence of height difference on the flow of the gas phase, the distribution of particles of different Stokes number (St), and the erosion of the aft wall and the downstream bottom wall, while the cavity is placed horizontally.

2. Problem description and setting

Fig. 2 shows the 2-D computational domain used in the present study in accordance with that of Fessler and Eaton [17]. The channel height S is 40 mm and the height of leading wall H is 26.7 mm. To obtain the developed turbulence flow upstream of the cavity, the computational domain starts at 32S upstream and ends at 35H downstream. The origin of the coordinates is set as the top point of the leading wall. For brevity, all the structural and positional parameters mentioned below are normalized by H. The cavity length (L) is maintained as a constant with a value of 3, which means that the downstream bottom wall starts at the x coordinate of 3. The height difference between the leading and aft walls (h) varies from 0 to 1. The working temperature is set as 25 °C, and the working pressure is assumed as 1.01×10^5 Pa (standard atmospheric pressure). The gas centerline velocity is 10.5 m/s and the gas flow Reynolds number is 18,400. The spherical sand is used as the particle with a density of 2500 kg/m^3 and mass flux ratio of 0.2. The pipe walls are assumed to be smooth, and their material is carbon steel with a Brinell hardness of 140.

The Stokes number, a dimensionless number that reflects the behavior of particles in a flow, is used to study the motion of particles. According to Fessler and Eaton [18], a fluid time scale (τ_f) based on an approximate large-eddy passing frequency and a modified particle time scale (τ_p) for a non-negligible Reynolds number is used to estimate the particle Stokes number, shown as

$$St = \frac{\tau_p}{\tau_f} = \frac{\rho_p d_p^2 / 18\mu \left[1 + 0.15\mathrm{Re}_p^{0.687}\right]}{5H/U_C} \tag{1}$$

where ρ_p is the particle density, d_p is the particle diameter, μ is the kinematic viscosity of the carrier fluid, U_c is the gas centerline velocity, and Re_p is the particle Reynolds number defined as

$$\mathrm{Re}_P = \frac{\rho d_p \left|\mathbf{V_p} - \mathbf{V}\right|}{\mu} \tag{2}$$

where $\mathbf{V}$ and $\mathbf{V}_p$ are the velocity vectors of the fluid and the particle. According to the results of Fessler and Eaton [18], for the calculation of the Stokes number, the average particle slip velocity ($|\mathbf{V_p} - \mathbf{V}|$) is assumed as 0.6 m/s. In this paper, the investigated particle diameters are 15, 50, and 150 μm with corresponding St values of 0.12, 1.2, and 9, respectively.

3. Simulation modeling

The Eulerian–Lagrangian finite element modeling method is used in this study. The fluid is treated as a continuous phase and solved by the Navier–Stokes equations, while particles are treated as a discrete phase and solved by Newton's second law. Additionally, two-way fluid–particle coupling is applied between the continuous phase and discrete phase. The commercial software FLUENT (Ansys, Inc., Canonsburg, PA, USA) is employed in the numerical calculation. Details of the models are presented in the following Sections.

3.1. The continuous phase

Since the inlet velocity of the air is very low and the Mach number is considerably less than 0.3, the carrier fluid is set as an incompressible gas with a density of 1.225 kg/m^3 and dynamic viscosity of 1.79×10^{-5} Pa s. The dynamics of incompressible flow is governed by the time-varying conservation of mass and momentum, namely the incompressible Unsteady Reynolds-Averaged Navier–Stokes (URANS) equations. As the cavity structure contains free shear flow, the shear-stress transport (SST) model, developed by Menter [19], is used to calculate the turbulence flow of the continuous phase as well. The SST model blends the robust and accurate formulation of the k–ω model in the near-wall region with the free-stream independence of the k–ε model in the far field. The conservation equations for the continuous phase are given by

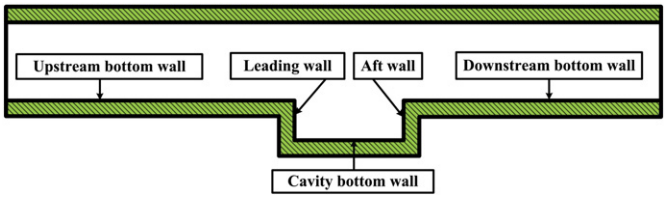

Fig. 1. Structure of an ideal cavity whose leading wall and aft wall have the same height.

$$\nabla \cdot \mathbf{V} = 0 \tag{3}$$

$$\frac{\partial \mathbf{V}}{\partial t} + \nabla \cdot (\mathbf{VV}) = -\frac{1}{\rho}\nabla P + \nabla \cdot \boldsymbol{\tau} + \mathbf{g} - \sum \mathbf{F} \tag{4}$$

$$\frac{\partial k}{\partial t} + \nabla k\mathbf{V} = \nabla \cdot \frac{1}{\rho}\left(\mu + \frac{\mu_t}{\sigma_k}\right)\nabla k + P_k - \beta^* k\omega \tag{5}$$

$$\frac{\partial \omega}{\partial t} + \nabla \omega\mathbf{V} = \nabla \cdot \frac{1}{\rho}\left(\mu + \frac{\mu_t}{\sigma_\omega}\right)\nabla \omega + P_\omega - \beta\omega^2 + 2(1-F_1)\frac{1}{\omega\sigma_{\omega 2}}\nabla k \nabla \omega \tag{6}$$

where $\boldsymbol{\tau}$ is the stress tensor modeled, $\Sigma\mathbf{F}$ are the forces between the continuous phase and the particles, P_k represents the generation of turbulence kinetic energy, μ_t is the turbulent viscosity, P_ω represents the production of ω, σ_k and σ_ω are the turbulent Prandtl numbers for k and ω, F_1 is the blending function, and β^* and β are equation coefficients.

3.2. The disperse phase

Since we have a dilute particle phase, we assumed that the inter-particle collisions and particle rotations can be neglected in the calculation procedure. According to Clift [20], the Cartesian coordinate form of the governing equation of the particle motion can be written as:

$$\frac{d\mathbf{V_p}}{dt} = \left(1 - \frac{\rho}{\rho_p}\right)\mathbf{g} + \sum \mathbf{F} \tag{7}$$

where the first term on the right-hand side is the gravity force, and the second term includes the drag force ($\mathbf{F}_D$), virtual mass force ($\mathbf{F}_{vm}$), pressure gradient force ($\mathbf{F}_P$), Magnus lift force ($\mathbf{F}_M$), Basset history force ($\mathbf{F}_B$), Saffman's lift force ($\mathbf{F}_S$), thermophoretic force ($\mathbf{F}_T$), and Brownian force ($\mathbf{F}_{Br}$). The considerations for including or neglecting these hydrodynamic forces in our numerical model are discussed below.

The drag force is the force that acts on the particle in a uniform pressure field when there is no acceleration of relative velocity between the

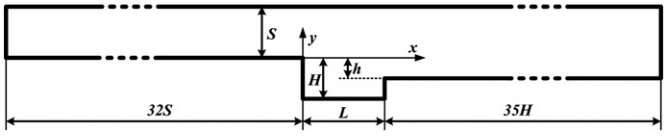

Fig. 2. Schematic structure of the computational domain.